

Distributed Anomaly Detection and PMU Data Recovery in a Fog-computing-WAMS Paradigm

Kaustav Chatterjee and Nilanjan Ray Chaudhuri
School of Electrical Engineering and Computer Science
The Pennsylvania State University, PA 16801, USA

Abstract—With rapid increase in the number of Phasor Measurement Units (PMUs) in the electric grid, massive volumes of monitoring data are expected to overwhelm the data pre-processors at centralized computing facilities. This, along with the requirements of lower latency and increased resilience to data anomalies advocates for distributed architectures for data conditioning and processing. To that end, in this paper, we present a fog-computing-based hierarchical approach for distributed detection and correction of anomalies in PMU data. In our proposed approach, each fog node, responsible for real-time data pre-processing, is dynamically assigned a smaller group of PMU signals with similar modal observabilities using software-defined-networking (SDN). The SDN controller residing at a central node feeds on the modeshapes estimated from the signals recovered at each fog node, for running the PMU-grouping algorithm. Grouping ensures adequate denseness of each signal set and guarantees data recovery under corruption. Also, the grouping is soft-real-time, infrequent, and triggered only upon a change in operating condition and therefore, heavily relieves the computational burden off the central node. The effectiveness of the proposed approach is demonstrated using simulated data from the IEEE 5-area 16-machine test system.

I. INTRODUCTION

Ever since the blackout in the northeastern United States in 2003, the number of PMU deployments in the grid has progressively increased with significant investments from the federal government and private utilities. Under the U.S. Department of Energy's Smart Grid Demonstration Initiative, this number increased over ten-folds between 2009 and 2015 [1] and continues to grow further. This, on one hand, has opened up opportunities for a range of critical applications like – wide-area oscillation monitoring, real-time event detection and classification, parameter estimation and model validation among others, but at the same time has left independent system operators (ISOs) and utility companies struggling to comprehend on how to harvest, process, and effectively utilize these huge volumes of real-time data coming from multiple large power system interconnections [2]. As of April 2020, there are over 400 PMUs in PJM alone spitting data at 30 samples-per-second [3]. This along with another 400 PMUs from neighbouring regional transmission organizations (RTOs) generate approximately 42 GB of data daily [3] which needs to be stored, processed, and analyzed at its central control location. With the continuing data explosion, this will soon become untenable under the current centralized monitoring architecture.

Thus motivated, theoretical advances have been made towards transitioning to a wholly or partially decentralized monitoring paradigm. To that end, distributed algorithms for modal estimation and damping control, state estimation, and voltage

control have been developed [2], [4], [5] concurrently with developments in protocols and communication modalities for network optimization and algorithm implementation [6]. This has been further fueled by the emergence of fog-computing [7]–[9] as a promising technology that brings cloud-computing applications closer to the physical devices at the network edge. In a more formal definition, a fog node [9] is a virtual platform that provides computational, archival, and networking facilities and is typically, but not exclusively located at the edge of a network. In the parlance of wide-area monitoring, a local software or hardware phasor data concentrator (PDC) along with all its computing and data routing capabilities would loosely qualify for this.

Apart from distributing the computational burden, fog computing is also expected to address the issues of latency, bandwidth, data privacy, and reliability from single-point failures [2]. While these merit decentralization, one major challenge before a fully distributed wide-area monitoring system (WAMS) would be to ensure resilience from data anomalies. In any measurement system, sustained missing data values, spurious outliers, and data inconsistencies are commonplace [10]. Further, as outlined in [11], a dedicated intranet-based communication network in NASPInet architecture is not immune to cyber attack. Anomalies, if not detected and corrected, can adversely affect the outputs of the estimation and control algorithms leading to potential errors in decision making [12]. Traditionally, in a system with partial observability, bad data detection and correction is done in a centralized data pre-processor exploiting the spatio-temporal correlation of a large number of signal variables. In a distributed architecture, with fewer measurements pooled at each fog node, this can be challenging.

In a pursuit to address this, in this paper, we present an intelligent and adaptive PMU grouping strategy that combines signals with similar modal signatures at each fog-computing node (loosely speaking, at a local PDC). This, augmented by a Robust Principal Component Analysis (PCA)-based [13], [14] algorithm at each fog node, ensures accurate data recovery under corruption. Further, in our proposed approach, local PDCs work on the recovered data samples to generate individual modal estimates, which are then communicated with the neighboring PDCs to reach a global consensus on modes and modeshapes. Finally, these modeshapes from each local PDC is communicated to a super PDC wherein a clustering algorithm groups the signals with similar modal signatures. A central SDN controller then uses this clustering information to re-configure the PMU – local PDC communication graph downstream to physically implement

the grouping. Note, in our proposed approach, although the data recovery in each local PDC is performed in near-real-time, the grouping/clustering at super PDC happens only at intervals. This reduces the data processing burden at the central node by effectively distributing the computation among the fog nodes.

The rest of the paper is organized as follows. In Section II the problem is described in detail along with the theoretical reasoning behind signal grouping. In Section III the proposed approach is presented followed by a case study in Section IV. Lastly, in Section V we discuss the conclusions and scopes of future research.

II. PROBLEM DESCRIPTION AND BACKGROUND

Consider a total of n PMUs distributed across a transmission network. Let $z_i(t)$ be any signal measured by a PMU, this could either be the bus voltage or line current magnitude, angle, frequency, or rate-of-change-of-frequency (ROCOF) phasor at location where it resides. Owing to the chances of corruption from missing data, spurious outliers, and malicious injections, $z_i(t)$ may not be the true measurement, and thus, can be expressed as

$$z_i(t) = y_i(t) + e_i(t) \quad (1)$$

where, $y_i(t)$ is the true measurement and $e_i(t)$ is the additive signal corruption. Interestingly, if data from multiple PMUs are pooled together for a span of time, then due to spatio-temporal correlation in the measurements, the data-window thus formed can be said to span a subspace that is low-rank [15]. Also, at any instant, $e(t)$ – the vector of $e_i(t)$ -s for $i = 1$ to n can be assumed to be sparse with non-zero entries at locations of data corruption.

Therefore, the problem translates to decomposing the measurement vector $z(t)$ into a vector derived from a fixed low-dimensional subspace spanned by the time evolution of $y(t)$ and a vector with most entries as zero. In our previous works [16] and [17], this has been achieved for centralized monitoring, using a Robust PCA-based data recovery algorithm (discussed later in Section III-B). However, as discussed previously, for a distributed implementation this presents some unique challenges. First, the signal subspace derived from a smaller group of PMU signals aggregated at a fog node needs to be low-rank. And second, the signal subspace needs to be sufficiently dense, implying there cannot be sparse vectors in the span. Otherwise, the sparse corruptions in the direction of the ones in the span cannot be differentiated from the signal, and therefore, the decomposition would fail. Ensuring these two conditions are key to the question of guaranteeing the success of distributed data recovery.

Since we now appreciate that any arbitrary collection of PMU signals may not meet these conditions, let us delve towards exploring intelligent strategies for signal grouping. To do so, we need to understand what imparts denseness and low-rankness to a signal subspace. In [14], authors define denseness of a basis matrix \hat{U} as,

$$\kappa_s(\hat{U}) = \kappa_s(\text{range}(\hat{U})) = \max_{|T| \leq s} \left\| (\mathbf{I}_T)^H \text{basis}(\hat{U}) \right\|_2 \quad (2)$$

where, \mathbf{I}_T is the submatrix of the identity matrix \mathbf{I} containing the columns with indices in set T . Lower the value of κ_s , higher

is the denseness of the range space. Building on this measure, in [18] an analytical relationship was developed to express the denseness of a signal set in terms of the modal observabilities of the constituent signals. Further it was shown that, denseness can be increased (and consequently, κ_s decreased) by decreasing the variance in relative modal observabilities for each poorly damped mode. In other words, signals with observabilities in phase and magnitudes tightly bounded would result in a signal set sufficiently dense. Also, as a consequence of such signal grouping, numerical rank of any data window derived from the signal subspace should theoretically be 1.

Based on these results, our approach would therefore require grouping signals with similar modal observabilities for distributed data recovery. However, in regards to implementation, this raises a few questions – first, if the objective behind data recovery is to use it for resilient oscillation monitoring, how do we derive the modeshape information a priori for signal grouping; second, how do we estimate modes and modal observabilities in a decentralized way; third, in a distributed architecture, where do we run the grouping algorithm and how frequently do we need to re-group; and finally, how do we implement the grouping in terms of flexibly configuring the PMU-PDC communication. These will be answered as we discuss our proposed approach in the next section.

III. PROPOSED APPROACH

Building on the background and the discussions from the preceding section, we present a hierarchical approach for distributed anomaly detection and correction in wide-area monitoring systems. A schematic of the proposed method, shown in Fig. 1, is described next.

A. Communication between PMUs and Fog Nodes

To begin with, consider we have a set signals clustered in accordance to their modal signatures – details about the grouping will be discussed later in Section III-D. This clustering information at the central node is translated into switching rules for SDN. In our case, we consider an IP-based communication between PMUs and local PDCs (here, fog nodes) with network switches having the capability of routing traffic based on the logical rules enabled by SDN.

Unlike a traditional network, where the switches that forward packets also determine the network path to send those packets through, in an SDN, the decision-making functions are removed from the switches and handled by a centralized software, conventionally called the SDN controller. The switches downstream, receive instructions from this controller in an OpenFlow protocol [19]. For every data packet entering the network, the routing policy specifies the path that the packet should take to reach its destination. In addition to this, an endpoint policy is incorporated which defines whether two end nodes (here, PMUs and fog nodes/PDCs) should be able to communicate regardless of the path the communication flows. In summary, routing policy guides the data packet between network switches to reach a destination node, and the endpoint policy ensures that a desired data packet is dumped at a correct PDC [20]. Together, they implement the re-configurable communication network in Fig. 1 for grouping of PMU signals at respective fog nodes.

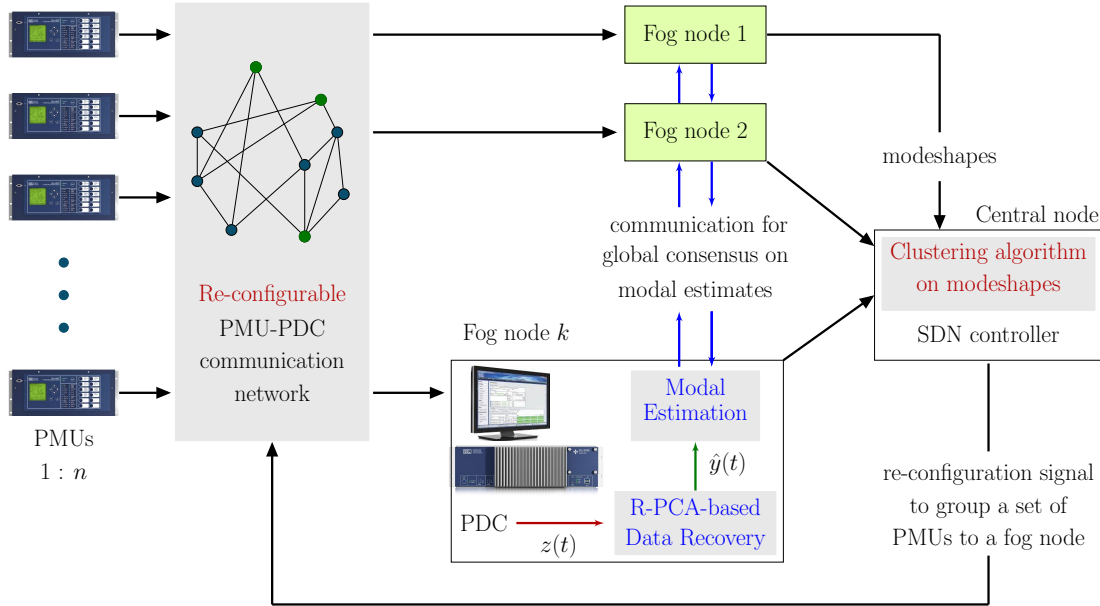


Fig. 1: Proposed hierarchical approach for distributed anomaly detection and data recovery.

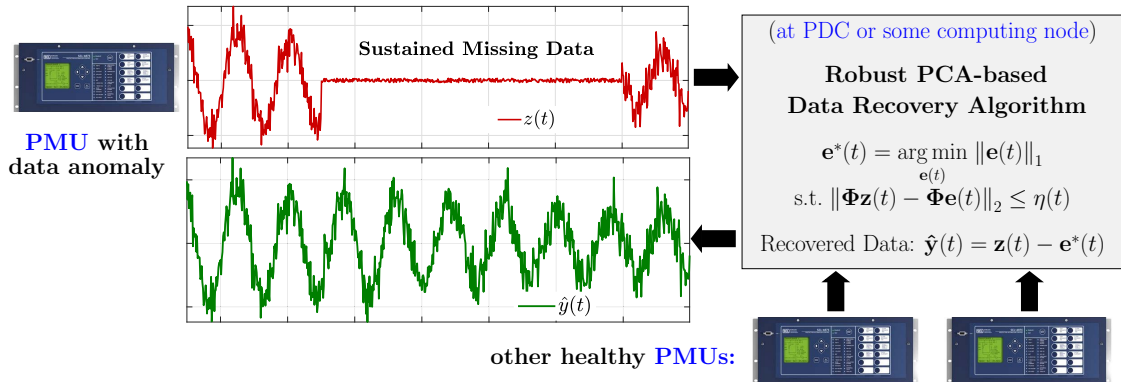


Fig. 2: Robust PCA-based anomaly detection and data recovery at a fog node.

At each fog node, local PDCs are responsible for time-aligning and sequencing the frames received from the PMUs and feeding it to a Robust-PCA-based data-preprocessor.

B. Anomaly Detection and Robust PCA-based Data Recovery at Fog Nodes

Let \mathcal{P}_ℓ denote the set of PMU signals grouped at fog node ℓ . Further define, $\mathbf{z}(t) = [z_{\ell_1}(t) \dots z_{\ell_j}(t) \dots z_{\ell_m}(t)]^T$ such that, signals with index $\ell_j \in \mathcal{P}_\ell \forall 1 \leq j \leq m$. The objective here, is to detect corruptions in $\mathbf{z}(t)$ and recover $\hat{\mathbf{y}}(t)$ as an estimate of $\mathbf{y}(t)$. The algorithm is summarized below.

Step 1: Perform a reduced singular value decomposition on a window of previously recovered samples:

$$\mathbf{Y} = [\hat{\mathbf{y}}(t - N\tau) \dots \hat{\mathbf{y}}(t - \tau)] \approx \hat{\mathbf{U}} \hat{\Sigma} \hat{\mathbf{V}}^H \quad (3)$$

Step 2: Project $\mathbf{z}(t)$ on to a space orthogonal to $\text{span}(\hat{\mathbf{U}})$

$$\gamma(t) = \Phi \mathbf{z}(t) = \Phi(\mathbf{y}(t) + \mathbf{e}(t)) = \Phi \mathbf{e}(t) + \nu(t) \quad (4)$$

where, $\Phi = \mathbf{I} - \hat{\mathbf{U}} \hat{\mathbf{U}}^H$ and $\Phi \mathbf{y}(t) = \nu(t)$ is a small numerical value mostly from noise and errors due to truncation in SVD.

Step 3: Estimation of sparse $\mathbf{e}(t)$ – posed as a LASSO-type convex optimization problem as follows

$$\mathbf{e}^*(t) = \arg \min_{\mathbf{e}(t)} \|\mathbf{e}(t)\|_1 \quad \text{s.t. } \|\Phi \mathbf{z}(t) - \Phi \mathbf{e}(t)\|_2 \leq \eta(t) \quad (5)$$

where, the thresholding term $\eta(t) = \|\Phi \hat{\mathbf{y}}(t - \tau)\|_2$ is updated every time-step.

For initialization, we either assume that the first few samples are uncorrupted, or use block processing techniques like [21] to recover the entire window of early samples. In either case, $\eta(0)$ initialized by $\|\Phi \mathbf{y}(0)\|_2$.

Step 3: A high value of $\|\mathbf{e}^*(t)\|_2$ is an indicator of data anomaly, and in such a case, the clean sample is recovered as:

$$\hat{\mathbf{y}}(t) = \mathbf{z}(t) - \mathbf{e}^*(t) \quad (6)$$

where, $\hat{\mathbf{y}}(t) = [\hat{y}_{\ell_1}(t) \dots \hat{y}_{\ell_j}(t) \dots \hat{y}_{\ell_m}(t)]^T$.

A schematic of the process is shown in Fig. 2. Next, using the recovered data points, system modes are estimated, and the signals are decomposed into the respective modal constituents.

C. Estimation of Modal Constituents at Fog Nodes

In this section, we discuss how modal constituents are extracted from the signals recovered at each fog node. As discussed, the modal constituents form the basis for signal grouping. Considering the small-signal dynamics of the system, any j^{th} signal recovered using the formulation described in Section III-B can be expressed as

$$\begin{aligned}\hat{y}_j(t) &\approx \sum_{i=1}^M \left\{ e^{\lambda_i(t)} \psi_{ji} + e^{\lambda_i^*(t)} \psi_{ji}^* \right\} = 2 \sum_{i=1}^M \operatorname{Re} \left\{ e^{\lambda_i(t)} \psi_{ji} \right\} \\ &= 2 \sum_{i=1}^M e^{\sigma_i t} \left\{ \operatorname{Re}(\psi_{ji}) \cos(\omega_{d_i} t) - \operatorname{Im}(\psi_{ji}) \sin(\omega_{d_i} t) \right\} \\ &\triangleq \Theta(t) \varphi_j\end{aligned}\quad (7)$$

where, M is the total number of poorly-damped modes in the system with $\lambda_i = (\sigma_i + j\omega_{d_i})$ being one such mode, and vectors

$$\begin{aligned}\varphi_j &= [\operatorname{Re}(\psi_{j1}) \quad \operatorname{Im}(\psi_{j1}) \quad \dots \quad \operatorname{Re}(\psi_{jM}) \quad \operatorname{Im}(\psi_{jM})]^T \\ \text{and } \Theta(t) &= 2 \begin{bmatrix} e^{\sigma_1 t} \cos(\omega_{d_1} t) & -e^{\sigma_1 t} \sin(\omega_{d_1} t) & \dots \\ e^{\sigma_M t} \cos(\omega_{d_M} t) & -e^{\sigma_M t} \sin(\omega_{d_M} t) & \dots \end{bmatrix}.\end{aligned}$$

At this stage of the problem, we are interested in the estimation of the modal observability ψ_{ji} – quantifying the extent to which any i^{th} mode is seen in the j^{th} signal, effectively its relative modeshape. To do so, we formulate a regression problem and adopt a recursive least squares approach for the estimation of the parameter vector φ_j . This is described next.

We define, $\hat{\varphi}_j(t)$ as an estimate of φ_j and $\epsilon_j(t)$ as the corresponding error in prediction of $\hat{y}_j(t)$. To begin with, $\hat{\varphi}_j(t)$ is initialized with zeros, and for every data sample $\hat{y}_j(t)$ recovered by the Robust-PCA algorithm thereafter, $\hat{\varphi}_j(t)$ is updated recursively using the estimate from previous time-step and the prediction error in the present time-step. Following steps are followed in the estimation process:

Step 1: Calculation of the prediction error

$$\epsilon_j(t) = \hat{y}_j(t) - \Theta(t) \hat{\varphi}_j(t-1) \quad (8)$$

Step 2: Computation of the gain

$$\mathcal{G}(t) = \frac{\mathbf{P}(t-1) \Theta^T(t)}{\Theta(t) \mathbf{P}(t-1) \Theta^T(t) + R_1} \quad (9)$$

where, \mathbf{P} is the covariance matrix of the prediction error and R_1 is the forgetting factor. For exponential convergence, R_1 is set to a value less than 1. In our problem, we use $R_1 = 0.9$ and the covariance matrix is initialized as $\mathbf{P}(0) = 10^4 \mathbf{I}$.

Step 3: Updation of the error covariance matrix

$$\mathbf{P}(t) = \frac{\{\mathbf{I} - \mathcal{G}(t) \Theta(t)\} \mathbf{P}(t-1)}{R_1} \quad (10)$$

Step 4: Updation of the parameter vector

$$\hat{\varphi}_j(t) = \hat{\varphi}_j(t-1) + \mathcal{G}(t) \epsilon_j(t) \quad (11)$$

Note that, the regressor vector $\Theta(t)$ is a function of σ_i -s and ω_{d_i} -s, and therefore, requires an accurate knowledge of these modal parameters. In our approach, we perform a distributed-Prony-based estimation of modal frequencies and damping ratios

using a variant of the distributed alternate direction method of multipliers (D-ADMM)-based algorithm discussed in [2]. This, in every iterative step, requires each fog node to share the locally estimated Prony coefficients with neighboring nodes to attain a consensus. Once the consensus is reached on the modes, the RLS-based estimation of φ_j is initiated, and $\Theta(t)$ is calculated for every time-step.

As t progresses, and new data points are available, $\hat{\varphi}_j(t) \rightarrow \varphi_j$ and $\epsilon_j(t) \rightarrow 0$. On convergence, the estimated values of $\hat{\varphi}_j$ -s are communicated to central node for signal grouping.

D. Signal Grouping at the Central Node

Next, we discuss the mechanism of signal grouping using modeshapes as features. For any j^{th} signal, a $2M$ -dimensional real feature vector F_j is formed from the estimated value of $\hat{\varphi}_j$ as shown

$$F_j = \hat{\varphi}_j = \begin{bmatrix} \operatorname{Re}(\hat{\psi}_{j1}) & \operatorname{Im}(\hat{\psi}_{j1}) & \dots & \operatorname{Re}(\hat{\psi}_{jM}) & \operatorname{Im}(\hat{\psi}_{jM}) \end{bmatrix}^T.$$

Following which, a naive- k -means clustering [22] is applied on the feature vectors to distribute the signal set into k groups. We define, \mathcal{P}_ℓ as the set of the signal-indices corresponding to any ℓ^{th} group. The iterative process for signal assignment to a group is described in eqns (12) – (13) below

$$\mathcal{P}_\ell^{(r)} = \left\{ j : \left\| F_j - \boldsymbol{\mu}_\ell^{(r)} \right\|_2^2 \leq \left\| F_j - \boldsymbol{\mu}_p^{(r)} \right\|_2^2 \quad \forall \quad 1 \leq p \leq k \right\} \quad (12)$$

$$\boldsymbol{\mu}_\ell^{(r+1)} = \frac{1}{|\mathcal{P}_\ell^{(r)}|} \sum_{j \in \mathcal{P}_\ell^{(r)}} F_j \quad (13)$$

where, r is the iteration count and $\boldsymbol{\mu}_p$ is the centroid of any p^{th} cluster. The algorithm is said to have converged when signal assignments to each group do not change and the cluster centroids converge to steady values.

Remarks: (1) Deciding on the number and size of the clusters is heuristic with an objective of maximizing the number of clusters with denseness coefficient κ_s (see Section II) below the threshold [18] desired for guaranteeing recovery.

Remarks: (2) Although data recovery and modeshape estimation runs at every time-step, the clustering need not. Strictly speaking, between successive time-steps modeshapes are not expected to change much unless the system is perturbed by a large disturbance leading to a change in operating point. Therefore, at quasi-steady-state, the clustering algorithm can run at infrequent intervals. However, it must run following every event like – clearing of faults, change of network topology, and detection of an outage.

As already discussed, the clustering information is finally encoded into routing rules at the SDN controller for re-configuring the PMU–PDC communication network.

Notice, this is a cyclic process – accurate estimation of modeshapes is contingent on correct data recovery, and successful data recovery further depends on a good signal grouping, which in-turn depends on the accuracy of modal estimation in the preceding step. At first, this might appear confusing, but can be easily tackled considering one uses the modeshapes calculated from reduced-order linearized models of the system (usually available from planning study) for the initial loop.

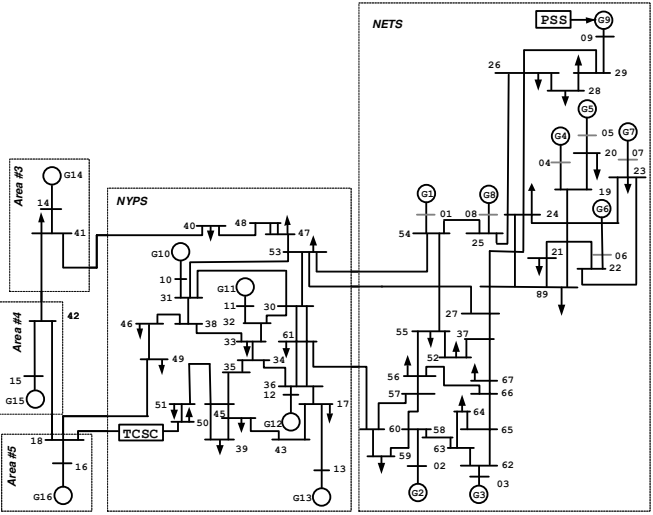


Fig. 3: IEEE 16-machine, 5-area New England - New York test system

IV. CASE STUDY

Consider the positive-sequence fundamental-frequency phasor model of the IEEE 16-machine, 5-area New England - New York test system as shown in Fig. 3. The machine and network data are obtained from [23]. An unit pulse is applied to the input of the TCSC and the variation in the bus voltage magnitudes thus obtained, are used in our analysis. The data is detrended by subtracting the pre-disturbance equilibrium from each signal.

Eigen-analysis of the system under nominal loading indicates presence of 4 poorly-damped modes with frequencies – 0.51 Hz, 0.39 Hz, 0.62 Hz and 0.79 Hz, and settling times – 28.8 s, 25.7 s, 18.1 s and 16.1 s, respectively. The signal grouping therefore, has to consider the modeshapes corresponding to these 4 modes.

The feature vectors derived from the modeshapes corresponding to these modes for each of the 69 voltage magnitude signals were grouped into 10 clusters using the framework discussed in Section III-D. Signals belonging to two such clusters, namely groups I and II are shown in Table I and their relative modeshapes in Fig. 4.

TABLE I: SIGNAL GROUPS I AND II

Group I	$ V_{19} $, $ V_{20} $, $ V_{21} $, $ V_{22} $, $ V_{24} $
Group II	$ V_{35} $, $ V_{39} $, $ V_{43} $, $ V_{44} $, $ V_{46} $

Next, to demonstrate the efficacy of the signal grouping, we corrupt $|V_{22}|$ and $|V_{39}|$ – arbitrarily one each from groups I and II (1-sparse corruption). We study three types of data corruption: (a) sustained missing data – modeled by replacing successive data samples with zeros, (b) noise injection – modeled by replacing blocks of actual data with random values in the signal range, and (c) malicious injection – artificially injecting a signal with completely different modal signature with an intention to mislead the monitoring process.

For each of the three corruption cases, data recovery as discussed in Section III-B, is performed for each signal group independently at their respective fog nodes. The recovered signal $\hat{y}(t)$, along its actual and corrupted counterparts: $y(t)$ and $z(t)$

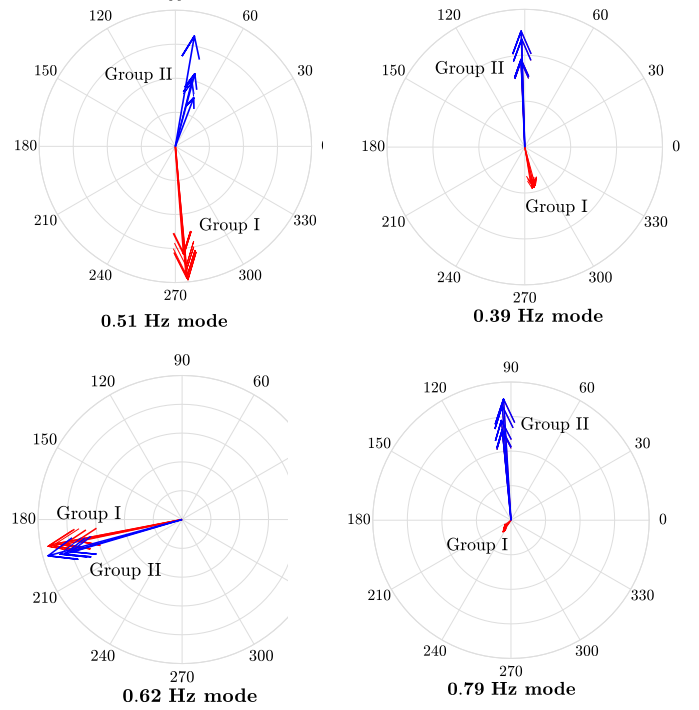


Fig. 4: Compass plot showing the clustering (or signal grouping) results on modeshapes for each of the 4 poorly-damped modes. Only groups I and II are shown – group I in red and II in blue.

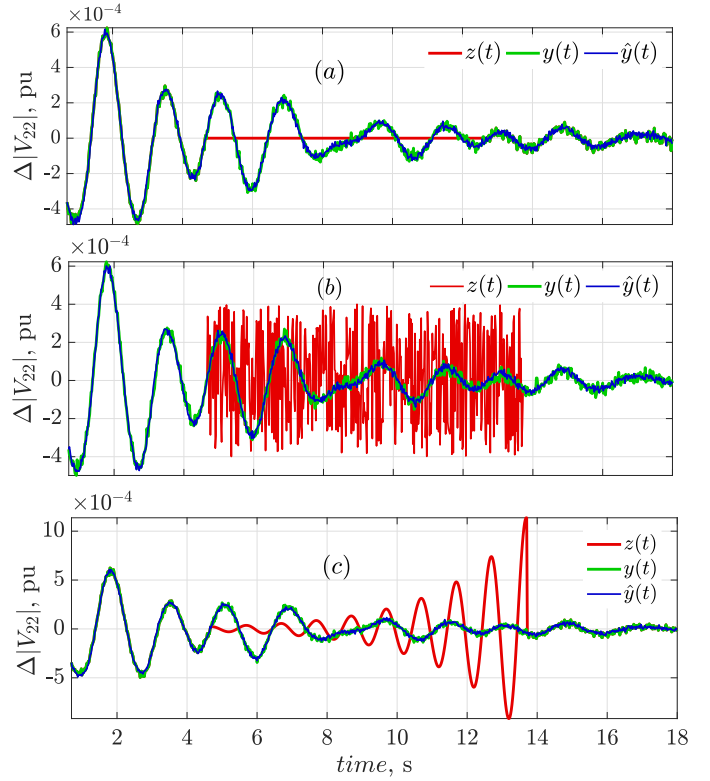


Fig. 5: Recovery of $|V_{22}|$ using signals in group I under different types of 1-sparse data corruption: (a) sustained missing data, (b) noise injection, and (c) malicious signal injection.

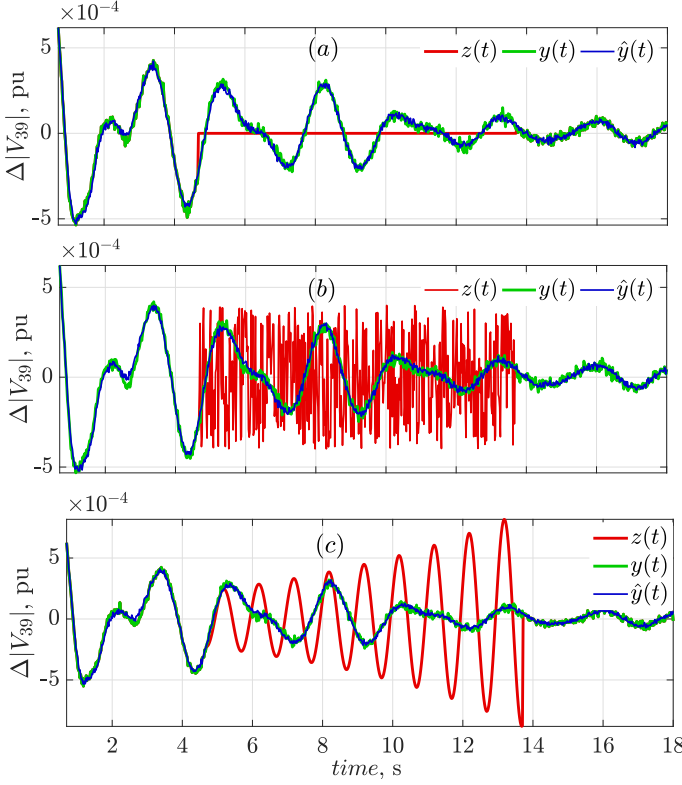


Fig. 6: Recovery of $|V_{39}|$ using signals in group II under different types of 1-sparse data corruption: (a) sustained missing data, (b) noise injection, and (c) malicious signal injection.

are shown in Figs. 5 and 6. The success of data recovery is evident from the plots. Further, the statistical dispersions – mean square error (MSE) and standard deviation of errors for the signal recoveries (compared to the uncorrupted ground-truth) are shown in Table II.

TABLE II: DISPERSION OF ERRORS IN SIGNAL RECOVERY

Corruption Type	Average MSE	Average Std. Dev.	Maximum MSE
Missing data	$2.64e - 6$	$1.84e - 7$	$1.55e - 5$
Noise injection	$1.55e - 6$	$2.28e - 7$	$1.12e - 4$
Malicious injection	$3.19e - 6$	$4.54e - 7$	$2.38e - 5$

V. CONCLUSION

In this paper, a fog computing-based hierarchical approach for distributed detection and correction of anomalies in PMU data streams was presented. In the proposed approach, PMU signals with similar modeshapes were grouped at a fog node wherein data recovery was performed using a Robust PCA-based algorithm. Signal grouping was performed at the central node (super PDC) using naive- k -means clustering on the signal modeshapes communicated from the fog nodes. Based on the results of clustering, the PMU-PDC communication was reconfigured using SDN to route the data packets from the targeted PMUs to their respective fog nodes.

ACKNOWLEDGMENTS

Financial support from the NSF grant under award CNS 1739206 is gratefully acknowledged.

REFERENCES

- [1] “Advancement of synchrophasor technology in projects funded by the american recovery and reinvestment act of 2009,” U. S. Department of Energy, Tech. Rep., 2016.
- [2] S. Nabavi, J. Zhang, and A. Chakrabortty, “Distributed Optimization Algorithms for Wide-Area Oscillation Monitoring in Power Systems Using Interregional PMU-PDC Architectures,” *IEEE Trans. Smart Grid*, vol. 6, no. 5, pp. 2529–2538, 2015.
- [3] PJM, *Learning Center*, <https://learn.pjm.com/energy-innovations/synchrophasors.aspx>, 2020 (accessed July, 20, 2020).
- [4] D. K. Molzahn, F. Dörfler, H. Sandberg, S. H. Low, S. Chakrabarti, R. Baldick, and J. Lavaei, “A Survey of Distributed Optimization and Control Algorithms for Electric Power Systems,” *IEEE Trans. Smart Grid*, vol. 8, no. 6, pp. 2941–2962, 2017.
- [5] L. Xie, D. Choi, S. Kar, and H. V. Poor, “Fully Distributed State Estimation for Wide-Area Monitoring Systems,” *IEEE Trans. Smart Grid*, vol. 3, no. 3, pp. 1154–1169, 2012.
- [6] A. Al-Fuqaha, M. Guizani, M. Mohammadi, M. Aledhari, and M. Ayyash, “Internet of Things: A Survey on Enabling Technologies, Protocols, and Applications,” *IEEE Commun. Surv. Tutor.*, vol. 17, no. 4, pp. 2347–2376, 2015.
- [7] F. Bonomi, R. Milito, J. Zhu, and S. Addepalli, “Fog Computing and Its Role in the Internet of Things,” in *Proceedings of the First Edition of the MCC Workshop on Mobile Cloud Computing*, New York, NY, USA, 2012, pp. 13–16.
- [8] S. N. Shirazi, A. Gouglidis, A. Farshad, and D. Hutchison, “The Extended Cloud: Review and Analysis of Mobile Edge Computing and Fog From a Security and Resilience Perspective,” *IEEE J. Sel. Areas Commun.*, vol. 35, no. 11, pp. 2586–2595, 2017.
- [9] E. M. Tordera, X. Masip-Bruin, J. Garcia-Alminana, A. Jukan, G. Ren, J. Zhu, and J. Farre, *What is a Fog Node A Tutorial on Current Concepts towards a Common Definition*, 2016. eprint: arXiv:1611.09193.
- [10] C. Huang, F. Li, D. Zhou, J. Guo, Z. Pan, Y. Liu, and Y. Liu, “Data Quality Issues for Synchrophasor Applications Part I: A Review,” *J. Mod. Power Syst. Clean Energy*, vol. 4, no. 3, pp. 342–352, Jul. 2016.
- [11] A. Ashok, M. Govindarasu, and J. Wang, “Cyber-Physical Attack-Resilient Wide-Area Monitoring, Protection, and Control for the Power Grid,” *Proc. IEEE*, vol. 105, no. 7, pp. 1389–1407, Jul. 2017.
- [12] K. Chatterjee, V. Padmini, and S. A. Khaparde, “Review of Cyber Attacks on Power System Operations,” in *2017 IEEE Region 10 Symposium*, Jul. 2017, pp. 1–6.
- [13] E. J. Candes and M. B. Wakin, “An Introduction To Compressive Sampling,” *IEEE Signal Processing Magazine*, vol. 25, no. 2, pp. 21–30, Mar. 2008.
- [14] C. Qiu, N. Vaswani, B. Lois, and L. Hogben, “Recursive Robust PCA or Recursive Sparse Recovery in Large but Structured Noise,” *IEEE Trans. Inf. Theory*, vol. 60, no. 8, pp. 5007–5039, Aug. 2014.
- [15] L. Xie, Y. Chen, and P. R. Kumar, “Dimensionality Reduction of Synchrophasor Data for Early Event Detection: Linearized Analysis,” *IEEE Trans. Power Syst.*, vol. 29, no. 6, pp. 2784–2794, 2014.
- [16] K. Mahapatra and N. R. Chaudhuri, “Online Robust PCA for Malicious Attack-Resilience in Wide-Area Mode Metering Application,” *IEEE Trans. Power Syst.*, vol. 34, no. 4, pp. 2598–2610, 2019.
- [17] K. Chatterjee, K. Mahapatra, and N. R. Chaudhuri, “Robust Recovery of PMU Signals With Outlier Characterization and Stochastic Subspace Selection,” *IEEE Trans. Smart Grid*, vol. 11, no. 4, pp. 3346–3358, 2020.
- [18] K. Chatterjee, N. R. Chaudhuri, and G. Stefopoulos, “Signal Selection for Oscillation Monitoring with Guarantees on Data Recovery under Corruption,” *IEEE Trans. Power Syst.*, pp. 1–1, 2020.
- [19] A. Goodney, S. Kumar, A. Ravi, and Y. H. Cho, “Efficient PMU networking with software defined networks,” in *2013 IEEE SmartGrid-Comm*, 2013, pp. 378–383.
- [20] H. Lin, C. Chen, J. Wang, J. Qi, D. Jin, Z. T. Kalbarczyk, and R. K. Iyer, “Self-healing attack-resilient pmu network for power system operation,” *IEEE Trans. Smart Grid*, vol. 9, no. 3, pp. 1551–1565, 2018.
- [21] K. Mahapatra and N. R. Chaudhuri, “Malicious corruption-resilient wide-area oscillation monitoring using principal component pursuit,” *IEEE Trans. on Smart Grid*, vol. 10, no. 2, pp. 1813–1825, 2019.
- [22] S. Lloyd, “Least squares quantization in PCM,” *IEEE Trans. on Inf. Theory*, vol. 28, no. 2, pp. 129–137, Mar. 1982.
- [23] N. R. Chaudhuri, “Wide-area Monitoring and Control of Future Smart Grids,” PhD thesis, Imperial College, London, U.K., 2011.